https://doi.org/10.37434/tpwj2021.06.02

# WELDING DISSIMILAR HIGH-STRENGTH NICKEL ALLOYS IN POLY- AND SINGLE-CRYSTAL COMBINATIONS

**K.A. Yushchenko, B.O. Zaderii, I.S. Gakh** and **G.V. Zviagintseva**
E.O. Paton Electric Welding Institute of the NAS of Ukraine
11 Kazymyr Malevych Str., 03150, Kyiv, Ukraine. E-mail: office@paton.kiev.ua

The paper deals with an important question, which arises at designing and improvement of the structure of gas turbine engines, in order to increase the operating parameters, cost characteristics and competitiveness: welding of dissimilar, multistructural high-temperature materials. Weldability assessment by the criteria of strength and crack resistance was performed. The main questions arising in welding high-temperature nickel alloys in dissimilar combinations: welding method, features of weld formation, chemical composition and structure, cracking susceptibility of welded joints and mechanical properties, are considered in the case of welding typical high-temperature materials widely used in aircraft engine building, namely EI698VD and ZhS26VI alloys with polycrystal and single-crystal structure, respectively. Methods to control the technological strength are established. Mechanical properties of welded joints produced in the temperature range of 20–1000 °C by different technology schemes are determined. 15 Ref., 5 Table, 7 Figures.

*Keywords: high-temperature nickel alloys, welding of dissimilar alloys, weld formation, chemical composition, single-crystal and polycrystal structure, crack resistance, properties*

Multicomponent complex-alloyed high-temperature nickel alloys (HTNA) with a poly- and single-crystal structure are the most common materials used for manufacture of parts of the hot section of modern gas turbine engines (GTE) [1–3]. However, improvement of their mechanical and service properties due to complex alloying and formation of a single-crystal structure leads to lowering of their processability, and, in particular, weldability [4, 5]. More over, the above materials feature high cost. Considering that individual components and parts of GTE hot section are exposed to nonuniform thermo-force impact along their entire length, their respective manufacture from different alloys using welding, is rational. The need to solve this problem becomes particularly acute when designing structures of the type of «blisk», «bling» and composite blades [6, 7]. It becomes necessary to determine the weldability and develop the technology of welding dissimilar and multistructural alloys. Difficulties arising in this case, alongside the problem of welding such alloys in the similar combination, are associated with the difference in their thermophysical and metallurgical characteristics. So, the difference in the melting temperature, ranges of crystallization, heat conductivity, fluidity, and specific density leads to problems in formation of sound welds and their structure. The difference in heat conductivity, coefficients of thermal expansion, elasticity moduli promotes formation of considerable welding stresses that leads to local deformation and crack initiation. The difference in chemical composition leads to formation of undesirable brittle chemical compounds, both as a result of simultaneous melting, and of diffusion processes during cooling.

The above-mentioned problems are becoming even more acute when producing multistructural welded joints of polycrystals with single-crystals.

Polycrystal wrought and powder HTNA are the main material for manufacture of turbine discs for high-pressure compressors, combustion chamber casings and other parts of GTE hot section [1, 8]. Among the commercial polycrystalline alloys the most widely used in aircraft engine building, are EI698-VD, EP742-PD, EK79-ND, EK151, EP975, Waspaloy, Astraloy, and Inconel 718 alloys.

Cast HTNA with single-crystal structure, as the more heat-resistant ones, are used mainly for manufacturing heavy-duty assemblies and parts, in particular, stator and rotor blades of GTE HPT. They are the most complex by their chemical composition and have up to 15 main alloying elements, not considering the microalloying elements [3, 9]. The commercial cast alloys commonly used in aircraft engine building include ZhS26, ZhS32, ZhS36, PWA1484, Rene'N6, CMSX-10, TMS-138, and TMS-162. While wrought alloys feature a higher fatigue resistance due to their fine-grained structure, cast alloys, owing to absence of high-angle grain boundaries in their structure and higher content of strengthening γ′-phase are characterized by higher values of high-temperature strength.

K.A. Yushchenko — https://orcid.ord/0000-0002-6276-7843, G.V. Zviagintseva — https://orcid.org/0000-0002-6450-4887

It should be noted that almost all the measures aimed at improvement of the alloy high-temperature strength, cause a deterioration of their weldability one way or another, that is related to lowering of their relaxation ability, increase of the level of localization and tempo of building-up of welding stresses, which can reach critical values in a broad temperature range. The main characteristics of the alloy weldability are proneness to cracking during welding and heat treatment, and degree of degradation of the structure and properties of the initial metal [5, 10].

The main problem of polycrystalline wrought HTNA are cracks in the HAZ, and for single-crystal cast alloys these are the so-called randomly oriented grains and cracks in the weld metal.

In welding HTNA with single-crystal structure, the above-mentioned problems, despite the absence of grain boundaries in the alloy structure, arise with equal severity that is related to more complex and saturated alloying [11]. More over, a not less important problem is the need to preserve the initial crystallographic orientation at minimum disorientation of structure elements and prevention of formation of grains of a different desorientation and cracks in the weld metal [12].

In welding of the above alloys to each other, in addition to the above-mentioned problems, it is also necessary to address the questions caused by dissimilarity of both the alloys proper, and of the third component of the welded joints — the weld of a different chemical composition and structure. It is obvious that in welding HTNA in the dissimilar, multistructural combination the problem of producing sound functional welded joints will become even more acute.

The objective of the work was establishing the possibilities and methods of producing sound multistructural welded joints of wrought (polycrystalline) HTNA with cast (single-crystal) ones.

**Investigation procedure and materials.** In order to perform investigations related to the possibility and technology of producing welded joints in a dissimilar combination, first of all, operative precision control of weld formation, its chemical composition and thermodeformational impact is required. As shown by the conducted analysis [6, 13], linear friction welding (LFW) is used to perform such operations, but this method requires expensive specialized fixtures, not available in the local factories of aerospace industry. More over, HTNA welded joints obtained by LFW method, are characterized by considerable structural inhomogeneity, presence of pore sequences and coarse carbide precipitates along the grain boundaries, and other defects that promotes cracking and lowering of the mechanical properties [13].

As shown by the experience of HTNA welding [14], the method of electron beam welding (EBW) is the most suitable for performance of such operations, considering the high power density, precision, heat source mobility and possibility of heat input control in a broad range and adaptability-to-manufacture. Joint formation in vacuum ensures a reliable protection of weld metal from oxidation, contamination by impurities, causing a change in the chemical composition, structural and physical homogeneity and deterioration of HTNA main properties. It should be noted that EBW equipment is manufactured in the Ukrainian enterprises.

Welding experiments and investigations were conducted on typical alloys, which are used in industry when designing GTE rotor structures — EI698VD wrought alloy with polycrystalline structure (rotor discs) and ZhS26VI cast alloy with a single-crystal or directional structure (blades). ZhS26VI single-crystal alloy produced at SC «Motor-Sich» was used to study the mechanical properties in the joints. Chemical composition and thermophysical characteristics of the studied alloys are given in Tables 1, 2. Samples of 50×25×2–3 mm size and thickness close to that of GTE real components were welded.

Welding modes were selected, proceeding from the need for complete penetration of the sample with root bead formation and weld form factor close to a unity. Here, lower overheating and deformations of the welded metal, and lowering of cracking probability are achieved.

A feature of fusion welding of dissimilar metals consists in that both the metals being welded form a

**Table 1.** Nominal chemical composition of welded HTNA, wt.%

| Alloy | C | Cr | Co | W | Mo | Ti |
|---|---|---|---|---|---|---|
| ZhS26VI | 0.13–0.18 | 4.3–5.3 | 8.0–10 | 10.9–12.5 | 0.8–1.4 | 0.8–1.2 |
| EI698VD | 0.03–0.07 | 13.0–16.0 | – | – | 2.8–3.2 | 2.35–2.75 |

**Table 1** (cont.)

| Alloy | Al | Nb | V | Fe | Si | Mn | B |
|---|---|---|---|---|---|---|---|
| ZhS26VI | 5.5–6.2 | 1.4–1.8 | 0.8–1.2 | ≤1.0 | ≤0.25 | ≤0.25 | 0.015 |
| EI698VD | 1.45–1.8 | 1.9–2.2 | – | ≤2.0 | ≤0.5 | ≤0.4 | 0.05 |

**Table 2.** Thermophysical characteristics of HTNA

| Alloy | Coefficient of heat conductivity λ, W/(m·°C), at $T$, °C | | | | | | | | | | | $T_L$, °C |
|---|---|---|---|---|---|---|---|---|---|---|---|---|
| | 25 | 100 | 200 | 300 | 400 | 500 | 600 | 700 | 800 | 900 | 1000 | |
| ZhS26VI | 7.95 | – | 10.7 | 12.1 | 13.6 | 14.6 | 16.3 | 18.0 | 20.0 | 22.6 | 24.7 | 1383 |
| EI698VD | – | 11.7 | 13.4 | 14.6 | 15.9 | 17.6 | 19.7 | 21.3 | 23.0 | 24.7 | – | 1440 |

common weld pool. Chemical composition of the thus formed alloy largely determines the nature of crystallization and structure of the weld metal, and welded joint properties. In its turn, chemical composition of the weld is determined by the share of each of the alloys in the weld metal, i.e. the ratio of the degree of their melting. The following welding schemes were used in order to produce welds with different chemical composition:

- fixed shifting of the welding beam from the butt axis to one of the samples being welded;
- asymmetrical scanning of the beam in the transverse direction;
- placing in the weld a technological insert of different thickness from the alloy of one of the samples being welded or an alloy of another composition.

Further analysis of chemical composition and structure of the produced welds showed that the most effective control of the weld composition is achieved in welding of dissimilar HTNA using a technological insert.

Certain difficulties were encountered at revealing the welded joint structure. This is related not only to different chemical composition of individual sections of the welded joint, but also to their different structural condition and phase composition, in particular, different content and dispersion of the main strengthening γ′-phase. The weld metal is a combination of the alloy sections of different structure, which is transitional between the polycrystal EI698 and single-crystal ZhS26 structures. Therefore, a steplike procedure was tried out for sequential detection of the structure of individual sections. In particular, the grain structure was revealed by chemical etching, and the dendritic and γ′-phases — by ion etching in VUP-4 unit. Moreover, a special etching time was selected in order to reveal the structure of each zone of the welded joint.

All the samples for experiments and investigations were cut out of the blanks by electric-spark method with subsequent grinding. The sections for metallographic investigations were prepared in Abramin grinding-polishing machine of Strues Company. The structure and chemical composition was analyzed, using optical microscope «Neophot-32» and electron microscope «CamScan» fitted with energy-dispersive local analysis system Energy-200. The weld quality and geometry were assessed by the appearance of the surface and the root, as well as by micro- and macrosections.

Mechanical characteristics of welded joints were determined by rupture testing of nonstandard samples cut out in the direction transverse to the weld axis. Cross-section of the sample working part was ~5 mm$^2$, its length was 28 mm. Testing was performed in the temperature range from room temperature to 1000 °C, considering that the working temperature of EI698 and ZhS26 alloys is equal to 650 and 1050 °C, respectively. Testing was conducted in MTS 810 unit at loading rate of 0.02 mm/s.

**Investigation results.** Weld formation is one of the issues arising in fusion welding of dissimilar metals. The main attention was given to establishing the influence of mode parameters at the above-mentioned welding schematics on the weld geometry and quality. It is known that of all the EBW energy parameters, the weld quality is the most strongly by affected beam power, position of its minimum cross-section (focus) relative the surface of the metal being welded, and welding speed. Optimum values of welding speed are determined, on one side, by minimum level of hydrodynamic disturbances, i.e. by the quality of weld formation, and on the other — by the conditions of ensuring the minimum weld width to lower the deformations, increase the cracking resistance, and preserve the content of volatile alloying components in the weld metal. Fulfilment of the first condition requires two times reduction of welding speed, and fulfilment of the second one necessitates its increase. Welding experiments were performed at the welding speed in the range of 10–120 m/h. At speeds below 10 m/g asymmetrical welds of a considerable width and complex (wine glasslike) geometry form with frequent burns-through of the metal being welded and undercuts (to 0.2 mm) from the side of ZhS26 alloy. Welding at the speed of ~120 m/h with small weld width leads to considerable undercuts, weld sagging, instability of formation and softening of the joint metal as a whole. Here, for each welding speed and scheme, and metal thickness, optimum values of current and beam focusing are different. Preheating in the range of 300–400 °C has only a slight influence on weld geometry: formation stability becomes somewhat higher and cracking probability decreases. At preparation for investigations the attention was focused on establish-

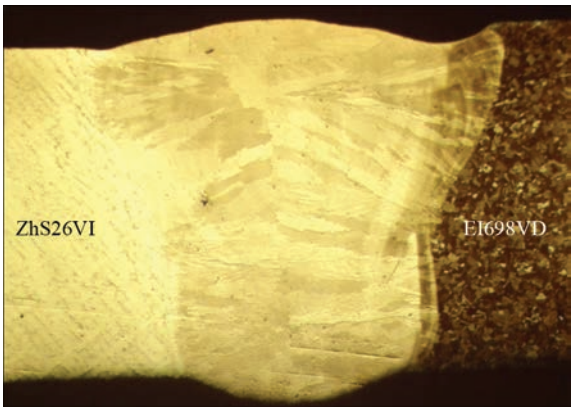


**Figure 1.** Shape of weld of 2.5 mm thick samples made at the speed of 53 m/h (×25)

ing the welding modes and schemes, ensuring through penetration and stable formation of welds of a symmetrical geometry.

Satisfactory formation was achieved at speed $v_w$ = = 50–60 m/h, beam focusing $\Delta I_f$ = +25 mA, power margin $I_b$ = 1.5–2.0 $I_{nom}$, $I_{nom}$ where is the value of current, at which through penetration is achieved, $\Delta I_f$ is the value of current in the focusing lens. In welding in such modes, the influence of the difference in thermophysical characteristics has practically no effect (Figure 1).

Here, with the above-mentioned «power reserve» of weld formation its geometry is less sensitive either to the change of speed, or (to a smaller degree) — to beam focusing. Going beyond the mentioned values of mode parameters $v_w \geq 88$ m/h, 15mA $\leq \Delta I_f \leq$ $\leq$ 35 mA, $I_b \leq 1.5\ I_{nom}$ leads to a noticeable change in weld geometry. The influence of $\Delta I_f$ is particularly noticeable at reduction of power reserve. Considering the above-said, samples for investigations were welded at increased speeds (~53 m/h) at considerable beam power reserve, that allowed somewhat widening the range of mode parameters for optimum weld formation. An even greater widening is in place in welding with beam scanning (Figures 2, 3). Formation of welds of a symmetrical geometry with fusion surfaces close to parallel ones (Figures 2, 3) and their stability and repeatability are facilitated that enhances the possibility of a more accurate control of the weld composition. In welding using technological inserts, scanning allows more uniform melting of the edges of the samples being welded and increasing the weld homogeneity. In addition, application of technological inserts greatly improves the weld quality and geometry (Figure 3). A positive effect is here achieved due to creation of a stable through-thickness channel, more laminar transfer of the weld pool melt into the tail part, absence of disturbance and uniform melting of the edges. Here, overheating of the HAZ is reduced, symmetrical transfer of molten metal in the

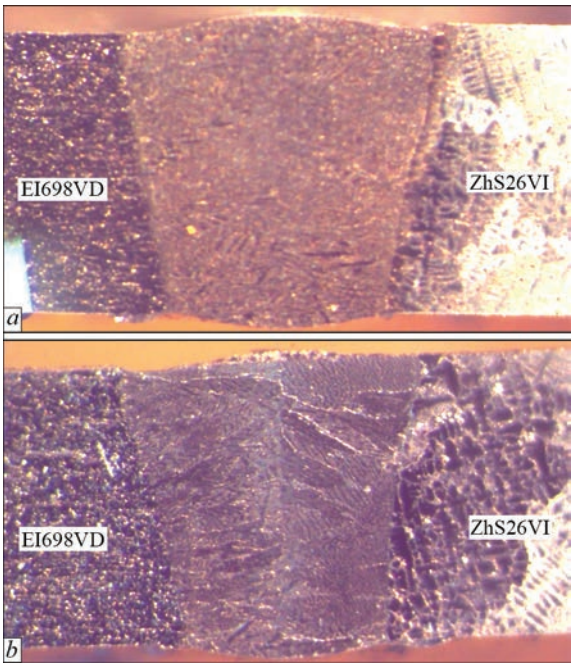


**Figure 2.** Macrosections of welded joints of ZhS26 and EI698 alloys, made at the same values of EBW mode parameters with asymmetrical beam scanning: *a* — on ZhS26 alloy; *b* — on EI698 alloy (×25)

weld pool, and stability and quality of weld formation are ensured.

Analysis of investigation results shows that the weld composition affects ZhS26 alloy more than EI968 alloy (Tables 2, 3) that is, obviously, associated with its greater surface melting due to lower melting temperatures, heat capacity and heat conductivity. Owing to the selected mode and methods of welding, the weld pool metal is intensively stirred, so the chemical composition both across and along the weld practically does not change. In all the considered variants, the weld metal is a high alloy, the chemical composition of which differs from either of the welded alloys (Table 5). In the case, when EI698 alloy components make up a greater fraction of the weld metal, a considerable increase, compared to the initial EI698, of

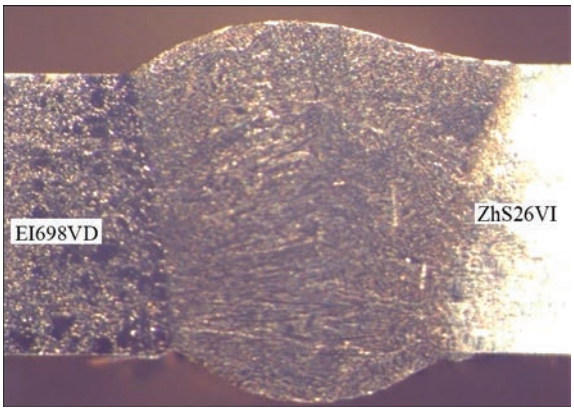


**Figure 3.** Macrosection of welded joints of ZhS26 and EI698 alloys made by EBW with technological insert from EI698 alloy (×25)

**Table 3.** Distribution of the main alloying elements in welded joints of EI698VD and ZhS26VI alloys (EDX analysis), wt.%

| Place of analysis | | Cr | Co | W | Mo | Ti | Al | Nb |
|---|---|---|---|---|---|---|---|---|
| Base metal | ZhS26 | 4.92 | 9.06 | 12.47 | 1.01 | 1.07 | 4.99 | 1.29 |
| | EI 698 | 14.77 | 0.32 | 0.72 | 3.02 | 2.68 | 1.34 | 2.2 |
| Weld metal | ZhS26 | 6.955 | 7.0 | 988. | 1.535 | 1.45 | 4.46 | 1.425 |
| | Стик | 8.32 | 6.08 | 8.06 | 1.94 | 1.6 | 3.75 | 1.66 |
| | EI 698 | 11.53 | 3.04 | 4.705 | 2.45 | 2.045 | 2.675 | 1.875 |

the content of aluminium, cobalt, and tungsten is observed at a certain decrease of the content of niobium, chromium, molybdenum and titanium. At maximum fraction of ZhS26 alloy, the change of chemical composition is smaller: the content of chromium, molybdenum, titanium and iron is somewhat increased, and a slight decrease of tungsten, cobalt, titanium and aluminium occurs, compared to initial ZhS26 alloy. At the same fraction of welded alloys in the weld metal, the alloying element content is not quite the arithmetic mean. More noticeable is the increase of tungsten, cobalt, and aluminium and lowering of titanium, molybdenum and niobium.

The observed chemical microinhomogeneity of the metal of welds, reflects the liquation, inherent to alloys with dendritic crystallization, when W, Re, Cr, Co alloying elements are concentrated on the dendrite axes, and Al, Ta, Nb — along the interdendritic interlayers.

The above-mentioned changes of the chemical composition have a significant influence, both on the microstructure, and phase composition of weld metal (Figure 4). In all the considered variants, the weld metal has a fine-dendritic directed structure of γ-matrix with dispersed precipitates of γ′-phase and carbides of different morphology and composition. The quantity of γ′-phase assessed by the aluminium coefficient, varies from 60 to 61 % for welds with maximum content of ZhS26 alloy and 45 to 46 % for ~50/50 composition and up to 22–25 % for welds with maximum content of EI698 alloy.

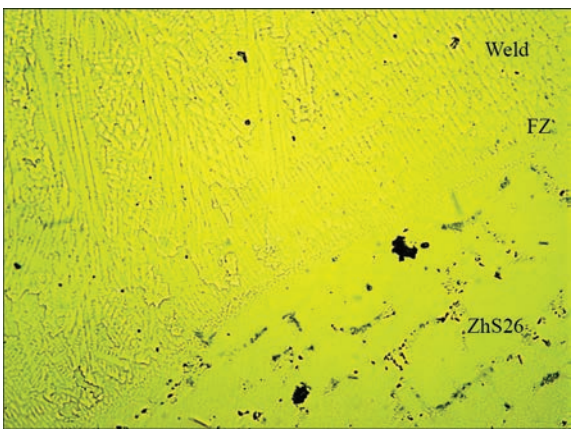


**Figure 4.** Microstructure (×200) of the transition zone of a section of metal of ZhS26 with EI698 alloy welded joint in the region of fusion with ZhS26

Despite the fact that the weld metal by its chemical composition differed from the initial alloy, at symmetrical crystallographic orientation of the sample of ZhS26 alloy near the fusion line, its clear inheritance is in place (Figure 4). The blocks of dendrites or grains of another crystallographic orientation different from the initial one, form only in the points of the change of fusion contour geometry or in the presence of chemical inhomogeneity of base metal. A grain structure with fine-dendrite filling oriented in the direction of maximum heat removal forms near the line of fusion with EI698 (Figure 5). Weld metal microstructure corresponds to chemical composition of high-nickel alloys (Figure 6), where the blocks of dendrites of one crystallographic orientation are outlined by secondary grain boundaries. In all the considered variants, the structure of weld metal in the transverse direction differs by noticeable heterogeneity. From the side of EI698 alloy this structure is characterized by presence of crystallites forming in individual grains or group of grains of close orientation in base metal (see Figure 5), whereas from the side of ZhS26 alloy first a section of 0.2 to 1.0 mm width is observed, which epitaxially inherits the initial crystallographic orientation of the single-crystal (Figure 4), and grains form only at a certain distance. Near the weld axis, where the crystallization fronts of ZhS26 and EI698 alloys meet, the usual, so-called rectilinear line of weakness is not formed, as due to nonstraightness of dendrite outlines, the grains kind of engage with each other (see Figure 6). It is obvious that formation of axial cracks was not observed in any of the experiments.

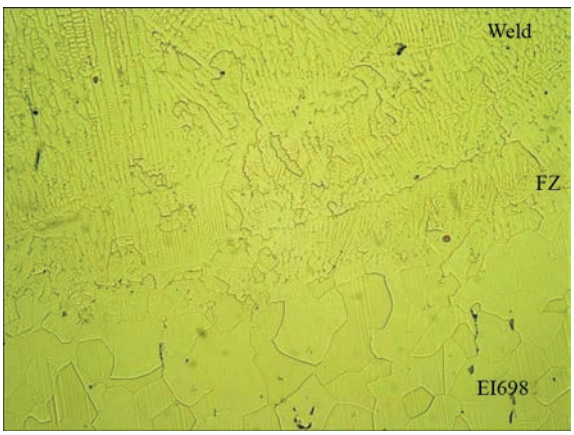


**Figure 5.** Microstructure (×200) of metal of ZhS26 with EI698 welded joint in the zone of fusion with EI698

It is well-known that the main disadvantage of high-alloyed HTNA which restrains their further development and wide acceptance by industry is their increased hot cracking susceptibility in fusion welding. This proneness is particularly obvious in alloys with increased high-temperature strength, which is mainly achieved due to higher and more complex doping of the alloys. Most of the authors [4, 10, 15] associate this proneness with the availability of two brittleness temperature ranges (ductility dip), which is where cracks form. The most critical are transverse hot cracks, forming in the brittleness temperature range (0.6–0.8 $T_s$), in which the weld metal is characterized by a small ductility margin at high ~ (0.8–0.9)$\sigma_{0.2}$ welding stresses. EI698 and ZhS26 alloys in a similar combination in fusion welding are also characterized by susceptibility to cracking in weld metal. In welded joints of EI698 alloy so-called underbead cracks are sometimes observed in the HAZ. ZhS26 alloy is more prone to formation of transverse cracks in welds. Here development of the latter is associated mainly with formation of high-angle grain boundaries.

It is obvious that these factors are manifested also in welding of the above-mentioned alloys in a dissimilar combination.

At consideration of welded joints of EI698 alloy with ZhS26 alloy made in the recommended modes, no cracks were revealed in EI698 HAZ (Figure 7). A positive role is played here by the geometry and small volume of weld metal. Transverse cracks were detected only in welds with maximum content of ZhS26 alloy components. Cracks are of interdendritic nature, more precisely, they pass along the interdendritic grain boundaries. Their formation is attributable to the weld chemical composition becoming very close to that of ZhS26 alloy, presence of high-angle grain boundaries, the latter being particularly pronounced at crystallographic orientation of the connecting single-crystal, far from high symmetry. Still, such joints have lower cracking susceptibility, compared to similar joints of ZhS26 alloy. It is obvious that the weld metal has better ductility, owing to higher purity, as to interstitial impurities of EI698 alloy and lower content of γ′-forming elements.

Fracture of welded joints at tensile testing of the samples in the temperature range of 20–500 °C (Tables 4, 5) mainly ran through the base metal of ZhS26 alloy. At temperature rise to 1000 °C, the fracture site shifts from ZhS26 base metal to EI698. Such a feature can be attributed to different content of γ′-phase in the welded joint components ~ 61 % in ZhS26, from ~ 60 to 25 % in the weld, depending on welding scheme, and ~ 22–20 % in EI698. Proceeding from the obtained results and considering the need to reduce the chemical heterogeneity of the welded joint, welding should be performed with predominant melting of EI698 alloy, or with application of technological inserts. The fracture site of the welded joint to a certain extent depends also on the crystallographic orientation of ZhS26 alloy that is related to anisotropy of single-crystal properties.

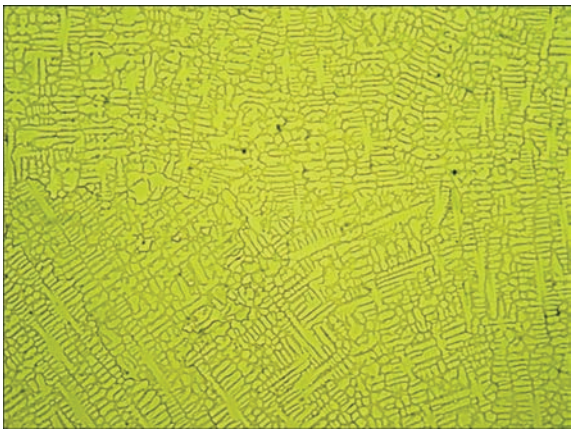

**Figure 6.** Microstructure (×200) of axial zone of weld metal in welded joint of ZhS26VI with EI698VD alloys

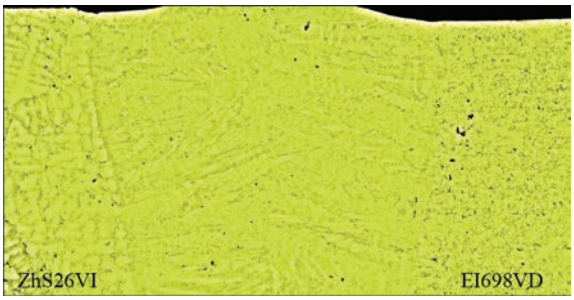


**Figure 7.** Welded joint of ZhS26VI with EI698VD alloys (maximum content of EI698 alloy components) (×50)

**Table 4.** Mechanical properties of welded joints of EI698VD with ZhS26VI alloys [001]

| $T_{test}$, °C | $\sigma_t$, MPa | $\sigma_{0.2}$, MPa | ψ, % | Fracture site |
|---|---|---|---|---|
| 20 | 980 | 860 | 10 | ZhS26 BM* |
| 500 | 1100 | 840 | 16 | ZhS26 BM |
| 650 | 1020 | 720 | 16 | EI698 BM |
| 750 | 890 | 680 | 18 | EI698 BM |
| 1000 | 269 | 200 | 18 | EI698 FZ** |

*Base metal. **Fusion zone.

**Table 5.** Mechanical properties of welded joints of dissimilar EI698VD with ZhS26VI HTNA alloys ([011] orientation)

| $T_{test}$, °C | $\sigma_t$, MPa | $\sigma_{0.2}$, MPa | ψ, % | Fracture site |
|---|---|---|---|---|
| 20 | 900 | 800 | 6 | ZhS26 BM* |
| 500 | 950 | 810 | 8 | ZhS26 BM |
| 650 | 980 | 830 | 10 | EI698 BM |
| 750 | 890 | 680 | 18 | EI698 BM |
| 1000 | 260 | 200 | 18 | EI698 FZ** |

*Base metal. **Fusion zone.

Thus, performed investigations show the possibility and methods of producing sound welded joints of dissimilar HTNA with mechanical properties on the level of one of the materials being welded.

**Conclusions**

1. Shown is the possibility of producing sound welded joints of HTNA in dissimilar combinations, including single-crystal with polycrystal alloys with respect to an urgent problem of creation of all-welded rotor structures and composite welded blades of GTE and GTU.

2. Schemes and modes of electron beam welding of dissimilar HTNA were developed and optimized, which allowed producing welded joints without cracks with mechanical properties on the level of those of base metal. At tensile testing in the temperature range of 20–650 °C, fracture of welded joints of EI698 alloy with ZhS26 alloy runs through the base metal of ZhS26 alloy, and in the temperature range of 700–1000 °C it passes through EI698 alloy, or in the zone of fusion of the weld with EI698.

3. In electron beam welding of EI698 alloy with ZhS26 alloy, the cracking susceptibility is reduced, compared to welds made in a similar combination, as a result of increase of relaxation ability of weld metal and of the joint as a whole, due to a controlled reduction of the content of γ′-forming elements (Al, Ti).

4. Improvement of the quality and properties of dissimilar mutlistructured joints of HTNA is achieved in welding:

- by electron beam method with controlled asymmetrical scanning of the beam;
- using a technological insert;
- with controlled content of γ′-forming elements.

The asymmetrical nature and amplitude of beam scanning, just as the insert dimensions, are determined mainly by the joint design and need to provide a certain chemical composition of the weld and its geometry.

5. Welds of EI698 alloy with ZhS26 alloy are characterized by finely-dispersed directed structure with dispersed precipitates of γ′-phase, carbides and carboborides of different morphology and chemical composition. Control of chemical composition and γ′-phase content of the welds allows producing welds with strengthening phase content from 60–62 to 22–25 %, owing to process scheme and parameters of electron beam welding process.

6. Obtained results of investigations of welding dissimilar and multistructural high-temperature wrought and cast single-crystal alloys can be the base for development of an industrial technology for creating all-welded rotor and stator assemblies and individual parts of GTE and GTU hot section.


1. Bratukhin, A.G. (2001) *Modern aviation materials, technological and functional peculiarities.* Moscow, AviaTekhInform 21st century [in Russian].
2. Sims, C., Stollof, N., Hagel, W. (1995) *Superalloys II. Heat-resistant materials for aerospace and industrial power plants.* Ed. by R.E. Shalin. Moscow, Metallurgiya [in Russian].
3. Stroganov, G.B., Chepkin, V.M. (2000) *Cast heat-resistant alloys for gas turbines.* Moscow, MATI [in Russian].
4. Morochko, V.P., Sorokin, L.I., Zybko, N.Yu. (1980) Weldability classification of high-temperature nickel alloys in EBM. *Avtomatich. Svarka*, **12**, 42–44 [in Russian].
5. Sorokin, L.I. (2003) Evaluation of cracking resistance in welding and heat treatment of high-temperature nickel alloys (Review). *Svarochn. Proizvodstvo*, **7**, 11–18 [in Russian].
6. XF9-1, the world's best standards fighter engine, has been completed. *Japan's Military Technology*, Interview with the Developer (Pt 1–2). BLOGOS (in Japanese). Retrieved 31 August 2019.
7. Kopelev, S.Z., Galkin, M.N., Kharin, A.A., Shevchenko, I.V. (1993) *Thermal and hydraulic characteristics of cooled gas turbine blades.* Moscow, Mashinostroenie [in Russian].
8. Bazileva, O.A., Arginbaeva, E.G., Turenko, E.O. (2012) Heat-resistant cast intermetallic alloys. In: Aviation Materials and Technologies. Moscow, *VIAM*, 57–60 [in Russian].
9. Kablov, E.N. (2001) *Cast blades of gas-turbine engines (alloys, technology, coatings).* Moscow, MISIS [in Russian].
10. Sorokin, L.I. (1999) Stresses and cracks in welding and heat treatment of high-temperature nickel alloys. *Svarochn. Proizvodstvo*, **2**, 11–17 [in Russian].
11. Yushchenko, K.A., Zadery, B.A., Zvyagintseva, A.V. et al. (2008) Sensitivity to cracking and structural changes in EBW of single crystals of heat-resistant nickel alloys. *The Paton Welding J.*, **2**, 6–13.
12. Yushchenko, K.A., Zadery, B.A., Karasevskaya, O.P. et al. (2006) Structural changes during welding process of single crystals of nickel supealloys in crystallographically asymmetric location of welding pool. *Novejshie Tekhnologii*, 28(**11**), 1509–1527 [in Russian].
13. Bychkov, V.M., Selivanov, A.S., Medvedev, A.Yu. et al. (2012) Investigation of weldability of high-temperature nickel alloy EP742 by linear friction welding method. *Vestnik UGATU*, 16(**7**), 52, 112–116.
14. Wiednig, C. (2014) Dissimilar electron beam welding of nickel base alloy 625 and 9 % Cr steel. *Procedia Engineering*, **86**, 184–194. https://core.ac.uk/download/pdf/82415005.pdf
15. Lippold, J.C., Cotecki, D.J. (2005) *Welding metallurgy and weldability of stainless steels.* Wiley interscience. A J.Wiley@ sons inc. Publ.


Received 19.04.2021